Polarization Effects on the Surface Chemistry of $PbTiO_3$-Supported Pt Films

Alexie M. Kolpak, Ilya Grinberg, and Andrew M. Rappe

The Makineni Theoretical Laboratories, Department of Chemistry, University of Pennsylvania, Philadelphia, Pennsylvania 19104-6323, USA

(Received 11 August 2006; published 16 April 2007)

To demonstrate a new paradigm of dynamical control of surface structure and reactivity, we perform density functional theory calculations of the adsorption of several molecules and atoms to the surface of ultrathin Pt(100) films supported on ferroelectric $PbTiO_3$. We show that reorienting the polarization direction of the substrate can dramatically change the chemisorption energies of CO, O, C, and N and alter the reaction pathways for dissociation of CO, O_2, N_2, and NO. We discuss the structural and electronic effects of a polarized substrate on the metal surface, and we suggest potential applications in tunable catalysis.

DOI: 10.1103/PhysRevLett.98.166101 PACS numbers: 68.43.Bc, 77.84.−s, 82.65.+r

Introduction.—As the ability to manipulate materials down to the atomic scale has increased with modern experimental techniques, the concept of tuning the properties of catalysts by optimizing their interactions with adsorbates at the atomic level has become increasingly realistic. One class of catalysts that has received a great deal of attention in this respect is that of oxide-supported metal catalysts, which are used in numerous industrial applications. Much progress has been made in determining the relationship between catalytic activity and the size, shape, and distribution of metal particles or films on a wide range of oxide supports [1–3]. Studies have also begun to elucidate the effect of the support material on the properties of the catalytic metal surface, showing that the surface polarization, acidity, and geometry, as well as the concentration of surface defects, all play a significant role in determining the behavior of the catalyst [3–9].

Based on these studies, we suggest that ferroelectric oxides will be excellent support materials, potentially offering dynamical control of surface structure and reactivity, with a wide range of available behavior in a single system. Ferroelectric materials have a spontaneous bulk polarization in the absence of an external field, and both the magnitude and the direction of the polarization can be changed by the application of an electric field. In addition, changes in polarization are accompanied by structural and chemical changes at the oxide-metal interface, resulting in a rich dependence of interfacial interactions on the oxide polarization. This suggests that ferroelectric oxide supports could greatly enhance the range of tunable parameters and enable external control of catalytic activity in real time.

Stadler has demonstrated that ferroelectric polarization can change the properties of supported metal films [10], and studies have also indicated that the ferroelectric transition can produce a significant effect on reaction rates on ferroelectric surfaces [11]. Other studies have suggested that ferroelectric materials can have a significant effect on the reactivity of supported metal catalysts. In a study of ethylene hydrogenation on $BaTiO_3$-supported Ni particles, the peak in turnover frequency was found to occur at the paraelectric-ferroelectric phase transition temperature of $BaTiO_3$, suggesting that the change in the polarization and/or structure of the underlying support was responsible for activating the Ni surface [12,13]. Another study found increased activity towards ethanol oxidation on Cu and Au surfaces supported by ferroelectric $LiNbO_3$ and attributed this activation to the presence of the electric field at the polarized $LiNbO_3$ surface [14]. In other work, ferroelectric supports have been used to generate acoustic waves, which have been shown to both activate and increase the selectivity of Ag, Pd, and Ni catalysts for alcohol oxidation and decomposition [15].

In the present study, we use density functional theory (DFT) [16,17] to systematically investigate the effects of a ferroelectric substrate on the electronic properties of a metal surface by studying ultrathin Pt films supported on a $PbTiO_3$(100) substrate. Examining the chemisorption behavior of CO, C, O, and N to the Pt surface as a function of Pt film thickness on two different $PbTiO_3$(100) surfaces, we show that switching from positive to negative polarization results in dramatic changes in chemisorption strength and site preference, particularly on monolayer-thick Pt films. In addition, we estimate trends in the dissociative chemisorption of CO, O_2, NO, and N_2 as a function of polarization direction and Pt thickness. Finally, we discuss the changes in electronic structure responsible for these effects, demonstrating that similar effects should be observed for other metals.

All DFT calculations were performed with the generalized gradient approximation [18,19] as implemented in the *ab initio* code DACAPO [20]. The structures were composed of two-unit-cell-thick $PbTiO_3$(100) films sandwiched between Pt(100) electrodes to form two PbO/Pt or TiO_2/Pt interfaces, as illustrated for PbO/Pt in Fig. 1. The interfacial Pt atoms are bound in the energetically favored registry, above the surface Pb and O ions in the former and above the surface oxygens in the latter. The structural and electronic properties of the interfaces were determined to be independent of the $PbTiO_3$ film thickness, as shown in Fig. 2; consequently, our system models the behavior of

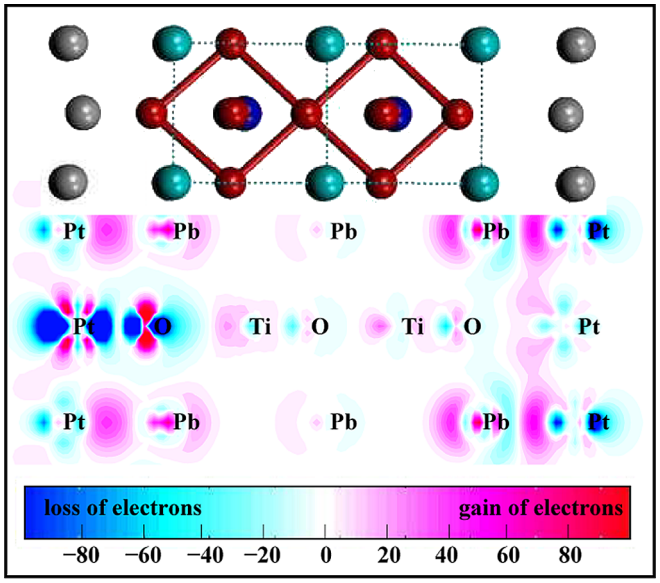

FIG. 1 (color online). Atomic structure and induced charge density (in me^{-}Å^3) for the PbO/Pt interfaces. Pb, Ti, O, and Pt atoms are shown as cyan, blue, red, and gray spheres, respectively. The P^- and P^+ interfaces are on the left and the right, respectively. The contour plot axes are chosen to show the surface cations and anions and their bonds to the Pt atoms. The general trends of interfacial charge rearrangement are similar for the analogous TiO_2/Pt interfaces; for illustration, see Ref. [22].

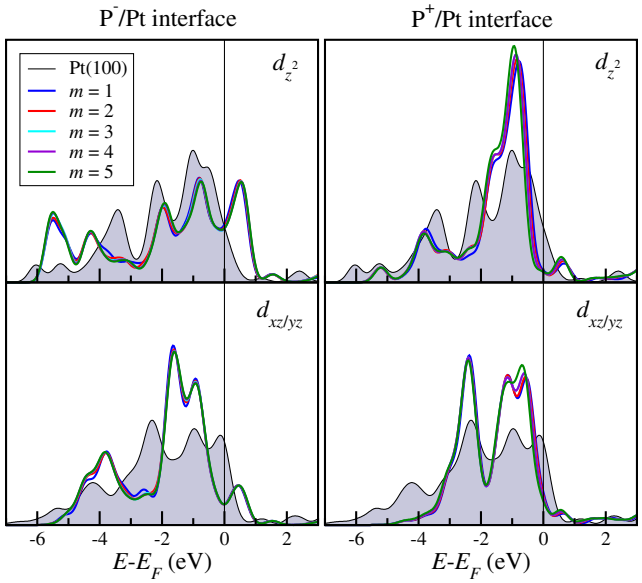

FIG. 2 (color online). Platinum d_{z^2} and $d_{xz/yz}$ DOS as a function of $PbTiO_3$ film thickness for one monolayer of Pt above the P^- (left) and the P^+ (right) PbO-terminated $PbTiO_3$, with $m = 1$–5 oxide unit cells. The shaded gray curve shows the corresponding DOS for Pt(100). Regardless of the $PbTiO_3$ film thickness, the electronic structure of the interfacial Pt layer remains almost constant, suggesting that the Pt surface reactivity is also independent of the substrate thickness.

Pt films supported on substrates ranging from ultrathin to thick $PbTiO_3$ films. A slab geometry with periodic boundary conditions is used, with the in-plane lattice constant fixed to the theoretical $PbTiO_3$ value of 3.86 Å to model epitaxial growth on a $SrTiO_3$ substrate, upon which Pt(100) films have been successfully grown [21] ($SrTiO_3$ is a common experimental substrate which is lattice matched to ferroelectric $PbTiO_3$). Slabs were separated by more than 20 Å in the direction perpendicular to the surface, and a dipole correction was applied in the center of the vacuum to remove artificial fields. All structures with and without adsorbates were relaxed completely until the force on each atom was less than 0.01 eV/Å. The films remained ferroelectric [22], with polarization perpendicular to the ferroelectric-metal interface and cation-anion displacements of 80%–90% of the computed bulk values.

The effects of the polarization on molecular and atomic chemisorption energies on the Pt surface are dramatic, as shown in Figs. 3(a)–3(d). Similar results were observed for both PbO- and TiO_2-terminated supports, but we focus here on PbO/Pt for brevity. For CO, C, O, and N, switching the $PbTiO_3$ polarization from P^+ to P^- induces changes of 0.4–0.8 eV in the chemisorption energy on a monolayer-thick Pt film. As the Pt film thickness is increased, the changes in chemisorption energy with respect to Pt(100) become less dramatic but remain significantly greater than the error bar of 0.01 eV in our DFT calculations. As Fig. 3 demonstrates, the effects of the substrate polarization extend over a length scale greater than the screening length of Pt (≈0.5 Å), indicating the importance of polarization-induced changes in atomic structure and chemical bonding in addition to the polarization charge. Interestingly, the adsorption behavior does not vary monotonically with respect to film thickness but oscillates relative to Pt(100) values, with opposite phases for the P^+ and P^- interfaces, suggesting Friedel oscillations in the metal screening.

The oxide substrate polarization also has a significant effect on adsorption site-preference energies. While the site-preference energies converge to the unsupported Pt(100) values more quickly than the chemisorption energies, the changes can be quite dramatic on a single-layer Pt film [Figs. 3(e)–3(h)]. For instance, CO chemisorption is equally strong on the top and bridge sites on unsupported Pt(100), but an underlying P^+ interface induces a 0.55 eV bridge site preference. Flipping the polarization direction destabilizes adsorption at the bridge site, resulting in a top-site preference of 0.23 eV above the P^- interface.

Such changes in molecular potential energy surfaces on the Pt film can have a large effect on reaction kinetics. Catalytic reactions with diatomic reactants are usually modeled as two successive processes: dissociative chemisorption followed by associative desorption. If chemisorption is too favorable, then all of the sites become covered with one reactant, blocking out the other. If it is not favorable enough, then the paucity of the reactant slows the reaction. This makes the overall rate of a surface catalytic process sensitive to the dissociative chemisorption energy. Therefore, the plot of reaction rate versus

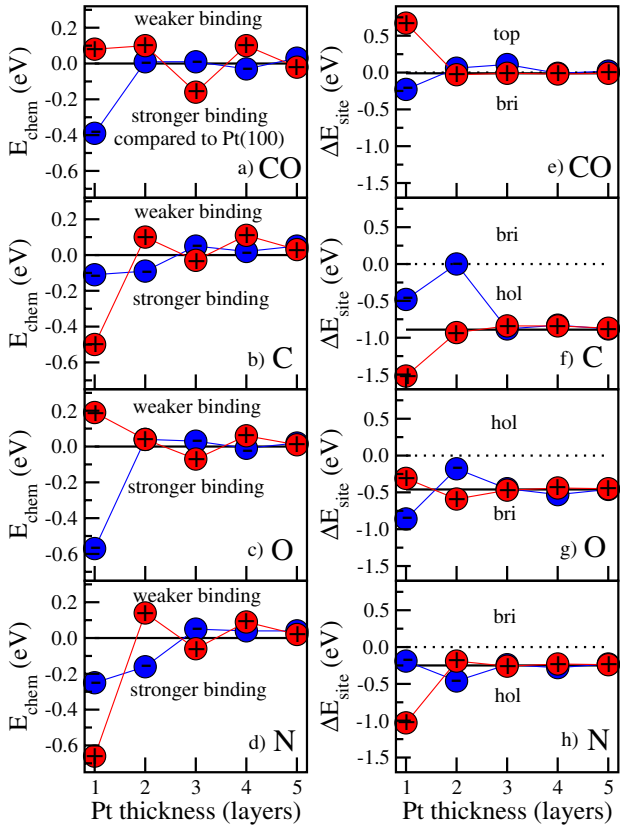

FIG. 3 (color online). (a)–(d) Chemisorption energies for CO [26], O, C, and N as a function of polarization direction and Pt thickness for the PbO/Pt interfaces. Red plus signs indicate the P^+ interface, and blue minus signs represent the P^- interface. The zero of energy corresponds to E_{chem} on unsupported Pt(100). (e)–(h) Site-preference energies for CO, O, C, and N. The solid black lines give E_{site} for the adsorbates on unsupported Pt(100). Points above the dotted lines represent a change in the preferred bonding site relative to Pt(100).

dissociative chemisorption energy is sharply peaked and is known as a "volcano curve" [23,24]. When dissociative chemisorption of the diatomic molecule is the rate-determining step, it can be shown that the peak of the volcano occurs when the free energy $A_{\text{diss}} \approx 0$ or $E_{\text{diss}} \approx T\Delta S$, where T is the temperature and S is the entropy lost during the dissociative chemisorption. This provides a simple criterion for optimizing the reaction rate over a given catalyst, such as by selecting the optimal T for a particular reaction. We propose that, by tuning E_{diss} through changes in the ferroelectric substrate polarization, it will be possible to optimize reaction rates for a wide range of desired temperature and pressure conditions.

To examine this possibility, we compute the dissociative chemisorption energies for CO, NO, O_2, and N_2 on $PbTiO_3$/Pt as a function of polarization and Pt film thickness. As the data in Table I show, the magnitude of E_{diss} depends strongly on the direction of the $PbTiO_3$ polarization, changing significantly with respect to both the oppositely polarized surface and the unsupported Pt(100) film. More importantly, Table I demonstrates that the presence of the polarized substrate can shift the dissociative adsorption energy significantly closer to the optimal range. For instance, the dissociative chemisorption energy for N_2 on Pt(100) is large and positive (+1.60 eV, unfavorable). Supporting the Pt on P^- TiO_2-terminated $PbTiO_3$ reduces E_{diss} to +0.74 eV, but switching the polarization direction to P^+ results in a negative (−0.12 eV, favorable) E_{diss}, near the optimum for this reaction. This effect could greatly accelerate the conversion of N_2 and H_2 into ammonia, since N_2 dissociation is the rate-determining step.

With CO dissociative chemisorption on a supported monolayer of Pt, the polarization direction of the substrate has the opposite effect: At the surface of both Pt(100) and Pt on P^+ PbO- and TiO_2-terminated $PbTiO_3$, CO dissociative chemisorption is unfavorable but becomes favorable for a negative substrate polarization. Using Pt on a negatively polarized $PbTiO_3$ could be useful in synthetic fuel production via Fischer-Tropsch synthesis, in which CO dissociation is the rate-determining step [25] in the formation of liquid hydrocarbons from H_2 and CO. The difference between polarization dependences of CO and N_2 E_{diss} can be explained by the interaction of the preferred binding sites of the constituent atoms with the substrate polarization, as discussed below.

Conversely, changing the substrate polarization can shift E_{diss} away from the optimal range, preventing or inhibiting dissociation below a certain temperature. Based on the kinetic model described above, we can compute the changes in optimal reaction temperature due to polarization switching to illustrate this effect [23]. For reactions involving O_2 dissociative adsorption, reversing the oxide substrate polarization leads to a ≈ 440 K shift in the optimal reaction temperature over one monolayer of Pt. This is due to the large difference in O_2 E_{diss} between the positively and negatively polarized substrates (Table I). Such an effect may be desirable for inhibiting corrosion and limiting catalyst degradation due to surface oxidation of the reactive metal.

Changes in chemisorption energy and E_{diss} are strongly correlated with site preference and $PbTiO_3$ substrate po-

TABLE I. Computed dissociative chemisorption energies on $PbTiO_3$/Pt as a function of polarization direction for monolayer and bilayer Pt films. Energies are in eV.

Interface	**P**	n_{Pt}	CO	O_2	NO	N_2
PbO/Pt	P^+	1	0.23	−1.24	−1.77	0.28
PbO/Pt	P^+	2	0.68	−1.54	−1.12	1.88
TiO_2/Pt	P^+	1	0.21	−1.20	−1.95	−0.12
TiO_2/Pt	P^+	2	0.48	−1.56	−1.27	1.60
PbO/Pt	P^-	1	−0.14	−2.76	−2.12	1.10
PbO/Pt	P^-	2	0.49	−1.54	−1.42	1.28
TiO_2/Pt	P^-	1	−0.07	−2.54	−2.19	0.74
TiO_2/Pt	P^-	2	0.65	−1.38	−1.21	1.54
Pt(100)			0.54	−1.62	−1.30	1.60
Pt(111) [23]			0.37	−2.17	−1.27	1.37

larization. For simplicity, we concentrate on monolayer results. Figures 3(b)–3(d) show that adsorption on the P^+ surface is more favorable for the C and N atoms, while O strongly prefers P^-. Because the preference of O for P^- is the strongest, O-containing CO, O_2, and NO all have lower E_{diss} on the P^- PbO/Pt interface, while N_2 dissociates most readily over the P^+ surface (Table I). Figures 3(f)–3(h) also show that C and N atoms prefer hollow site adsorption, while the O atom favors the bridge site. This suggests that the P^- surface enhances E_{diss} if one or more of the constituent atoms preferentially adsorbs at a top or a bridge site. On the other hand, the P^+ surface lowers the dissociative chemisorption energy when both atoms of the dissociated molecule adsorb at hollow sites.

These trends can be understood by considering the effects of substrate polarization on the Pt d-band density of states (DOS). The d_{z^2} and $d_{xz/yz}$ Pt orbitals participate in bonding at the bridge site, while the $d_{xz/yz}$ contribution dominates for the hollow site. The DOS for a monolayer-thick Pt film (Fig. 2) shows a large increase in unfilled d_{z^2} states at the P^- surface. This is due to Pt d_{z^2} covalent bonding with O p_z at the P^- interface, which results in a low-energy bonding state around -5 eV and an unfilled antibonding state [9]. This covalent interaction can be seen clearly in Fig. 1 as well. The increased availability of empty states induced by these interfacial interactions strengthens top- or bridge-site chemisorption. By contrast, there are almost no free d_{z^2} states near the Fermi level for the P^+ surface. This weakens P^+ bridge-site adsorbate-metal bonding and makes O adsorption much stronger on P^- than on P^+. Figure 2 also shows that the $d_{xz/yz}$ orbitals shift upwards on the P^+ substrate, forming a large peak and increasing the availability of states just below the Fermi level, and thereby enhancing hollow site backbonding to adsorbates. In contrast, the peak in the $d_{xz/yz}$ orbitals shifts away from the Fermi level on the P^- substrate, decreasing the number of states available for backbonding. Consequently, the P^+ substrate is favored over the P^- substrate for hollow site C and N adsorption.

Our results have demonstrated the ability to significantly alter the surface electronic structure and catalytic activity of a metal thin film by switching the polarization of an underlying ferroelectric oxide. We have shown that the alterations are due to a combination of polarization, chemical, and structural changes and that these changes influence the metal surface properties to a distance of almost 1 nm away from the oxide surface. Furthermore, our analysis of the electronic structure suggests that these phenomena are not limited to Pt films but should be observable for a range of ferroelectric–transition-metal systems. Our results suggest the possibility of tuning the reactivity and selectivity of catalysts in real time by applying electric fields to ferroelectric oxide-supported films. Experimental studies have shown that the magnitude of the electric field required to flip the polarization (the coercive field) in $PbTiO_3$ films with Pt electrodes is within an experimentally feasible range. Based on the similar trends observed for TiO_2- and PbO-terminated substrates, other ferroelectric materials with smaller coercive fields, such as $Pb(Zr, Ti)O_3$ and $BaTiO_3$, are expected to behave similarly, providing further opportunities to optimize ferroelectric-supported metal catalyst systems for various applications. We hope that our results will stimulate further experimental and theoretical studies on such systems.

This work was supported by the Office of Naval Research, the Air Force Office of Scientific Research, and the National Science Foundation. Computational support was provided by the HPCMO and DURIP. A. M. K. was supported by Atofina.

[1] M. Valden, X. Lai, and D. W. Goodman, Science **281**, 1647 (1998).
[2] M. Haruta, Catal. Today **36**, 153 (1997).
[3] U. Heiz and E. L. Bullock, J. Mater. Chem. **14**, 564 (2004).
[4] K. Okumura, T. Kobayashi, H. Tanaka, and M. Niwa, Appl. Catal., B **44**, 325 (2003).
[5] S. Ichikawa, T. Akita, M. Okumura, M. Haruta, K. Tanaka, and M. Kohyama, J. Electron Microsc. **52**, 21 (2003).
[6] A. M. Doyle, S. K. Shaikhutdinov, S. D. Jackson, and H. J. Freund, Angew. Chem., Int. Ed. **42**, 5240 (2003).
[7] J. R. B. Gomes, F. Illas, N. C. Hernández, A. Márquez, and J. F. Sanz, Phys. Rev. B **65**, 125414 (2002).
[8] L. M. Molina and B. Hammer, Phys. Rev. Lett. **90**, 206102 (2003).
[9] V. R. Cooper, A. M. Kolpak, Y. Yourdshahyan, and A. M. Rappe, Phys. Rev. B **72**, 081409(R) (2005).
[10] H. Stadler, Phys. Rev. Lett. **14**, 979 (1965).
[11] G. Parravano, J. Chem. Phys. **20**, 342 (1952).
[12] C. Park and R. T. K. Baker, Chem. Mater. **14**, 273 (2002).
[13] C. Park and R. T. K. Baker, J. Phys. Chem. B **104**, 4418 (2000).
[14] Y. Inoue and Y. Watanabe, Catal. Today **16**, 487 (1993).
[15] N. Saito, Y. Yukawa, and Y. Inoue, J. Phys. Chem. B **106**, 10 179 (2002).
[16] P. Hohenberg and W. Kohn, Phys. Rev. **136**, B864 (1964).
[17] W. Kohn and L. J. Sham, Phys. Rev. **140**, A1133 (1965).
[18] J. P. Perdew, K. Burke, and M. Ernzerhof, Phys. Rev. Lett. **77**, 3865 (1996).
[19] B. Hammer, L. B. Hansen, and J. K. Nørskov, Phys. Rev. B **59**, 7413 (1999).
[20] http://dcwww.camp.dtu.dk/campos/Dacapo/
[21] A. J. Francis, Y. Cao, and P. A. Salvador, Thin Solid Films **496**, 317 (2006).
[22] N. Sai, A. M. Kolpak, and A. M. Rappe, Phys. Rev. B **72**, 020101(R) (2005).
[23] T. Bligaard, J. K. Nørskov, S. Dahl, J. Matthiesen, C. H. Christensen, and J. Sehested, J. Catal. **224**, 206 (2004).
[24] S. Dahl, A. Logadottir, C. J. H. Jacobsend, and J. K. Nørskov, Appl. Catal., A **222**, 19 (2001).
[25] Q. Ge and M. Neurock, J. Phys. Chem. B **110**, 15 368 (2006).
[26] S. E. Mason, I. Grinberg, and A. M. Rappe, Phys. Rev. B **69**, 161401(R) (2004).